A Non-Parametric Mixture Model for the fMRI Visual Field Map

Raymond G. Hoffmann[1], Nicholas Pajewski[2], Edgar A Deyoe[3], Daniel B Rowe[4]
[1]Quantitatiave Health Sciences, Pediatrics, Medical College of Wisconsin, Milwaukee, WI 53226
[2]Statistical Genetics, University of Alabama, Birmingham, AL 35294
[3]Radiology, Medical College of Wisconsin, 53226
[4]Biophysics, Medical College of Wisconsin, 53226

Abstract
The fMRI visual field map (VFM) is obtained by using a rotating-expanding visual target to identify the area of the retina that corresponds to activated visual cortex. Since fMRI data is (1) relative rather than absolute and (2) has a degree of noise that may mask the activation, identifying differences in VFMs requires a model that will differentiate changes in the underlying structure from differences due to imaging variability. The VFM produces a non-homogenous, non-isotropic set of points on a disk that includes irregular features like the blind spot. A non-parametric mixture model, using a Dirichlet prior on a space of 2D density functions, will be used to model the VFM under experimental conditions where part of the visual field is masked by a circular wedge. The posterior probability of the difference in the models, will be used to quantify the probable location of the wedge..

Key Words: Non-parametric, point process, Dirichlet prior, fMRI, imaging, spatial density

1. Introduction

The **visual field map** (VFM) is produced by mapping the active voxels of the visual cortex to a circular region corresponding to the points of a circular image. It is a dynamic option to the **Humphries** map that ophthalmologists use to evaluate visual acuity. The goal is to be able to use it to assess whether there are changes in the visual pathway due to a disease process, like migraine headaches, or where there have been changes due to an intervention, such as surgery for refractory epilepsy.

The VFM, like the retina of the eye is spatially inhomogeneous as well as not isotropic. There are more receptors near the center of vision which allows more sensitivity. There is a blind spot due to the presence of the optic nerve; although the visual cortex usually interpolates an image.

An fMRI scan of the optical cortex produces voxels, small cubes that can be "classified" as activated or not by whether the cortical blood flow correlates with a visual pattern thatchanges over time. By using an inverse transform the voxels in the visual cortex can be mapped onto a circular region corresponding to the cortex. This is the Visual Field Map. (figure 1, Brefczynski, 1999). This inverse mapping produces about 450 to 650 points in a Visual Field Map. Because of the "winner take all" rule for assigning activation, because the voxel may span two different regions of the visual cortex and because of the noise involved in a real fMRI signal, the resulting map has random points in the when it is assessed during different sessions. One descriptor of these random points is to model them as a point process with an underlying spatial spatial intensity. Noise in the signal may cause mapping to the wrong place or error in the assessment of activation.

The purpose of this paper is to develop a model that will have sufficient flexibility to map this irregular surface and provide a model for the underlying non-homogeneous intensity function. Then on the basis of this model we expect to be able to identify whether the map has changed from one scan session to another.

1.1 The Visual Field Map

The visual field diagram is formed by an inverse mapping of areas of the visual cortex to the retinotopic area stimulated by an array of visual targets. A series of circular annulus (doughnuts with a hole), expanding out from the center of the target plus a series of pie-shaped wedges rotating around the circular target are used to map the location on the retina to the location in the visual cortex. (figure 1, A Brefczynski, 1999).

Figure 1: The functional field map is constructed by (a) comparing the time lag of the repeated fMRI signal (b) with the annulus information and the rotating wedge information[1].

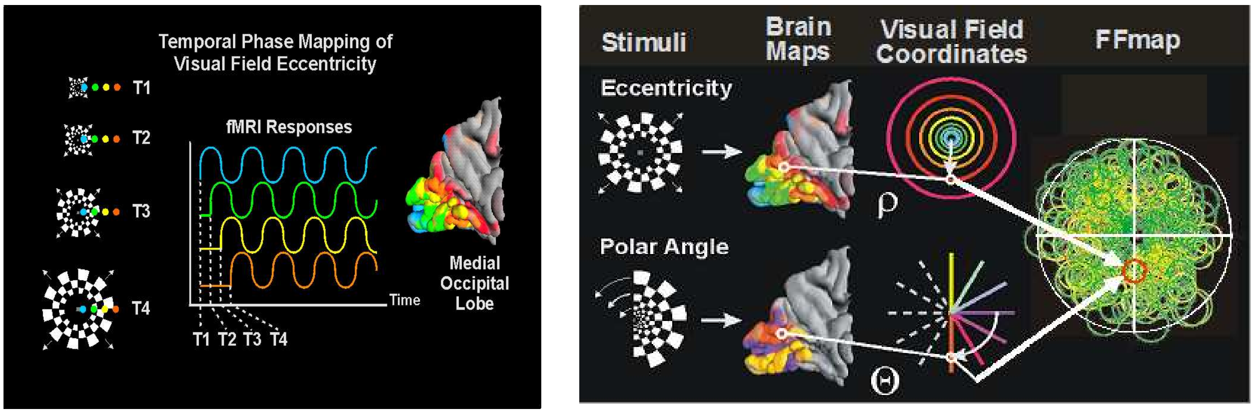

The size of the circle surrounding the center point of the VFM is sometimes taken to be a measure of uncertainty of the inverse map. For this paper, we will focus only on the mapping of the center point of the visual cortex to the VFM. Since the location of this point is not fixed under repeated scanning sessions, we will treat its location as a non-homogeneous point process.

1.2 Simulating Surgical Interventions on the VFM

The visual target that is used to obtain the VFM is composed of two parts. The first is a semicircular (180 degree) checkerboard pattern that rotates around a 360 degree circle. In order to “simulate” the effect of surgery, a wedge was cut out of the semicircular pattern. The second part of the target was a set of annuli (rings around the center of the visual field) that went from the center out to the edge of the visual field. Wedges were used to mask part of the visual field when the data was collected from a subject. The wedges were 0, 18, 27, 36, 45 and 90 degrees.n order to simulate differing effects of surgery. (figure 2). The differing angular size of the wedges was used to test the sensitivity of the of the methods to identify defects in the visual cortex.

Figure 2: The masks were wedges of 0, 18, 27, 36, 45 and 90 degrees

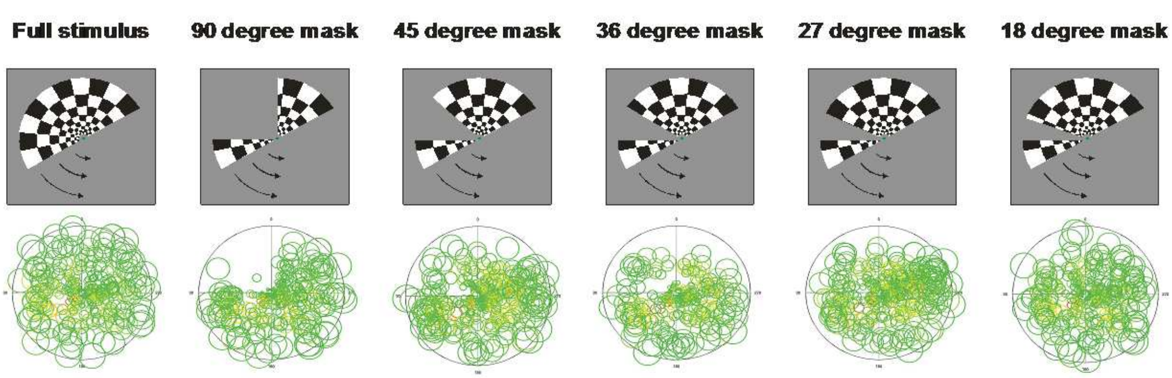

1.3 Additional Sources of Variability

Because of the "winner take all" rule for assigning activation and because the voxel may span two different regions and the noise involved in a real fMRI signal The resulting map has random points in the area of the wedge. Noise in the signal may cause mapping to the wrong place. Other difficulties in analyzing the data from the visual field map are first, changes in position between sessions can change the location of the points. Moreover, since fMRI provides a relative assessment of activation, the overall number of points activated depends on more than the underlying spatial intensity. Figure 3 show the difference in the number of points from 7 scans over a period of time with a fixed threshold for activation. Varying the magnitude of the threshold that defines activation can also changes the number of active points.

Figure 3: The Normalization Problem: 1 Subject at 7 Different Times

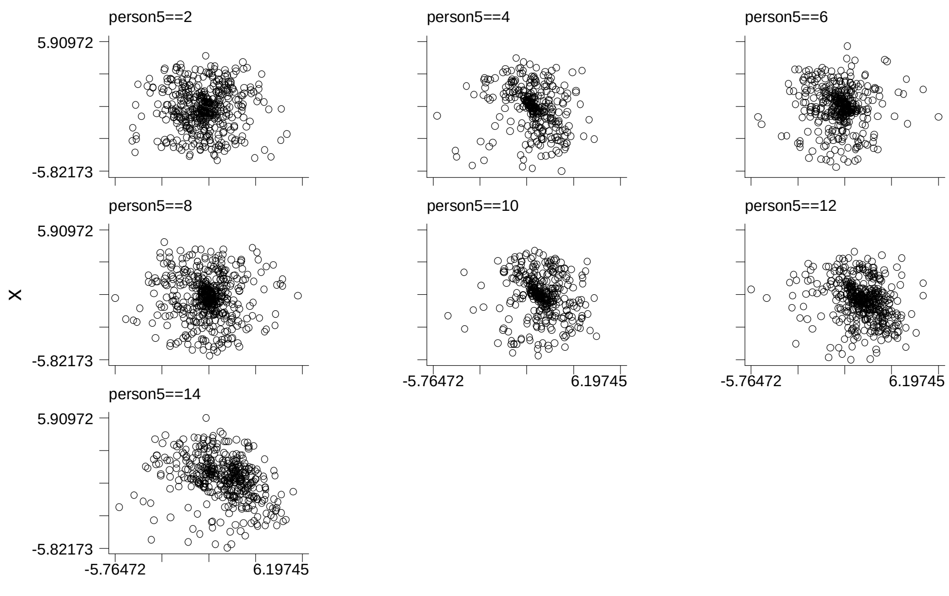

Number Of Activated Points

479
295
433
588
428
418
619

2. Statistical Methods

2.1 The Point Process Model

We will model the data with a point process. A point appears if it is above a threshold determined by correlating the fMRI signal with the pattern of the mask. The data is { $Y(s_i)$: $i = 1, \ldots N_k$ }, where s_i is the location of the point I and $Y(s_i) = 1$ if the point is activated.

The number of the events occurring within a finite region A can be modeled as a non-homogeneous Poisson process with mean

$$\int_A \lambda(s)ds$$

Given the total number of events N occurring within an area A, the intensity of the process is $\lambda(s)$. Parametric models for the spatial density for the VFM are developed in Hoffmann, 2007.

2.2 Evidence for a Mixture Model

Using a kernel smoother to empirically estimate the spatial intensity function (figure 4) suggests that the effect of removing a wedge from the spatial intensity can requires more than a single Poisson spatial intensity function. The irregular shape of the process also suggests that choosing a Poisson model may oversmooth the data. Thus we choose a non-parametric approach to modeling the underlying spatial intensity.

Figure 4: The smoothed data with wedges show multi-modal behavior

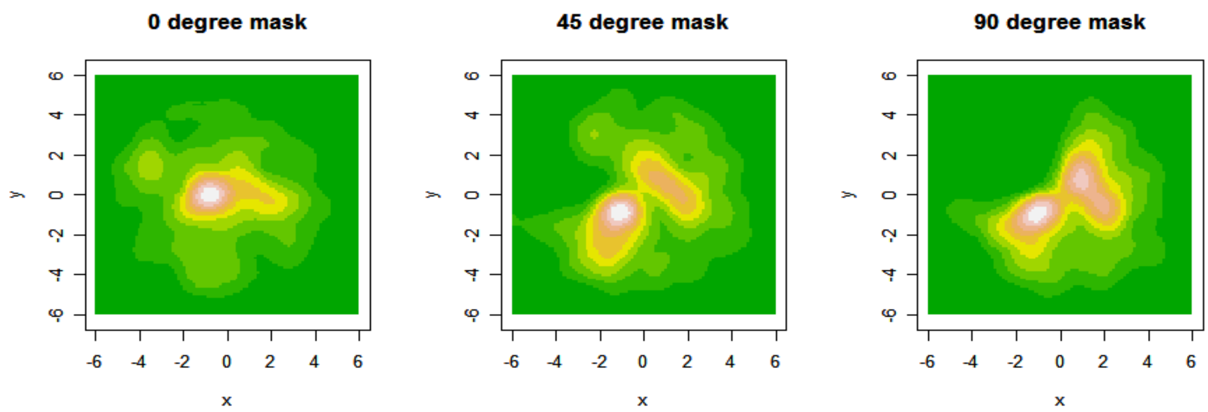

2.3 Using a Non-Parametric Model for the First Order Intensity

A non-homogeneous Poisson mixture model can be the weighted sum of more than one asymmetric Poisson intensity .

$$\lambda(s) = \sum_{i=1}^{3} \omega_i \exp\{\mu + \alpha_1 \tilde{x}_i + \alpha_2 \tilde{x}_i^2 + \beta_1 \tilde{y}_i + \beta_2 \tilde{y}_i^2 + \gamma_1 \tilde{x}_i \tilde{y}_i + \gamma_2 \tilde{x}_i \tilde{y}_i^2 + \gamma_3 \tilde{x}_i^2 \tilde{y}_i$$

where the ω_i are the weights applied to the components of the mixture and
where $\tilde{x}_i$ and $\tilde{y}_i$ are the distances from the centers of up to k - 3 mixture components .

Of course, the location of the centers also needs to be estimated.

2.1.1 The Dirichlet Process

A more generalized non-parametric spatial model is a Bayesian non-parametric spatial model where the number of components can vary as the number of points. Gelfand, Kottas and MacEachern (2005) introduced a **Dirichlet Process** as a prior mixing distribution on a family of densities DP(ν G_0). Central to the DP is the notion of a random probability measure on the space of distribution functions defined on the space Θ (with σ field B).

The family DP(ν G_0) is indexed by $\nu > 0$, a scalar precision parameter that controls the amount of clustering in the spatial measure on Θ and G_0 which is the specified base distribution. Although DP(ν G_0) is almost certainly discrete on the set of points, $Y(s_1) \ldots Y(s_N)$ it can be countably or uncountably infinite because of the order ($\aleph_1$) of the space we are modeling.

We will assume that G_0, the base density, is bivariate normal, with constant variance and covariance; however, this is not a necessary assumption (Duan, Guindani and Gelfand 2007). This gives the representation (it is almost surely discrete and finite)

$$\sum_{i=1}^{\infty} \omega_i \delta(\theta_i)$$

where θ_i is the location of the point mass, $\delta(\,)$ is the Dirac delta function, and the ω_i are the weights.

Because this gives a model that is too bumpy, a DDP, a Dependent Dirichlet Process, is actually used to smooth the process. Instead of having i represent each of the points in $\{Y(s)\}$, it represents the index value or the center of the bivariate $N(\mu, \Sigma)$ distribution, G_0. Another approach to eliminating the bumpiness is to convolve the DP(ν G) with a pure error process. This will create a process F with continuous support on $A \subseteq \Re^2$. The priors for the DDP are a 2D uniform circular prior on θ_i, the location parameter for each of the component clusters, an inverse gamma on the precision of the bivariate normal G_0 and a gamma prior on the mixing parameter ν.

2.1.2 Implementation

The DPpackage library in R implements Bayesian non-parametric density estimation with Dirichlet Processes, Dependent Dirichlet Processes, Polya Trees, Mixtures of Triangular distributions, and Random Bernstein polynomials. This package was developed by Alejandro Jara. It quite flexible and optimized to produces estimates quite rapidly. It took 5 to 10 minutes on a 1.33 GHz Pentium 3 to run a single chain with a 5000 point burn in, a skip factor of 20 and 10,000 points for the estimation.

3. Results

Figure 6 shows the results of fitting a DPM model to the points from a complete Visual Field Map. Note the marginal

Figure 6: The estimated posterior density for a visual field plot with a 0^o wedge
(a) the marginal density of x (b) the marginal density of y (c) a contour plot of the bivariate density and (d) a 3D perspective plot of the bivariate DPM density

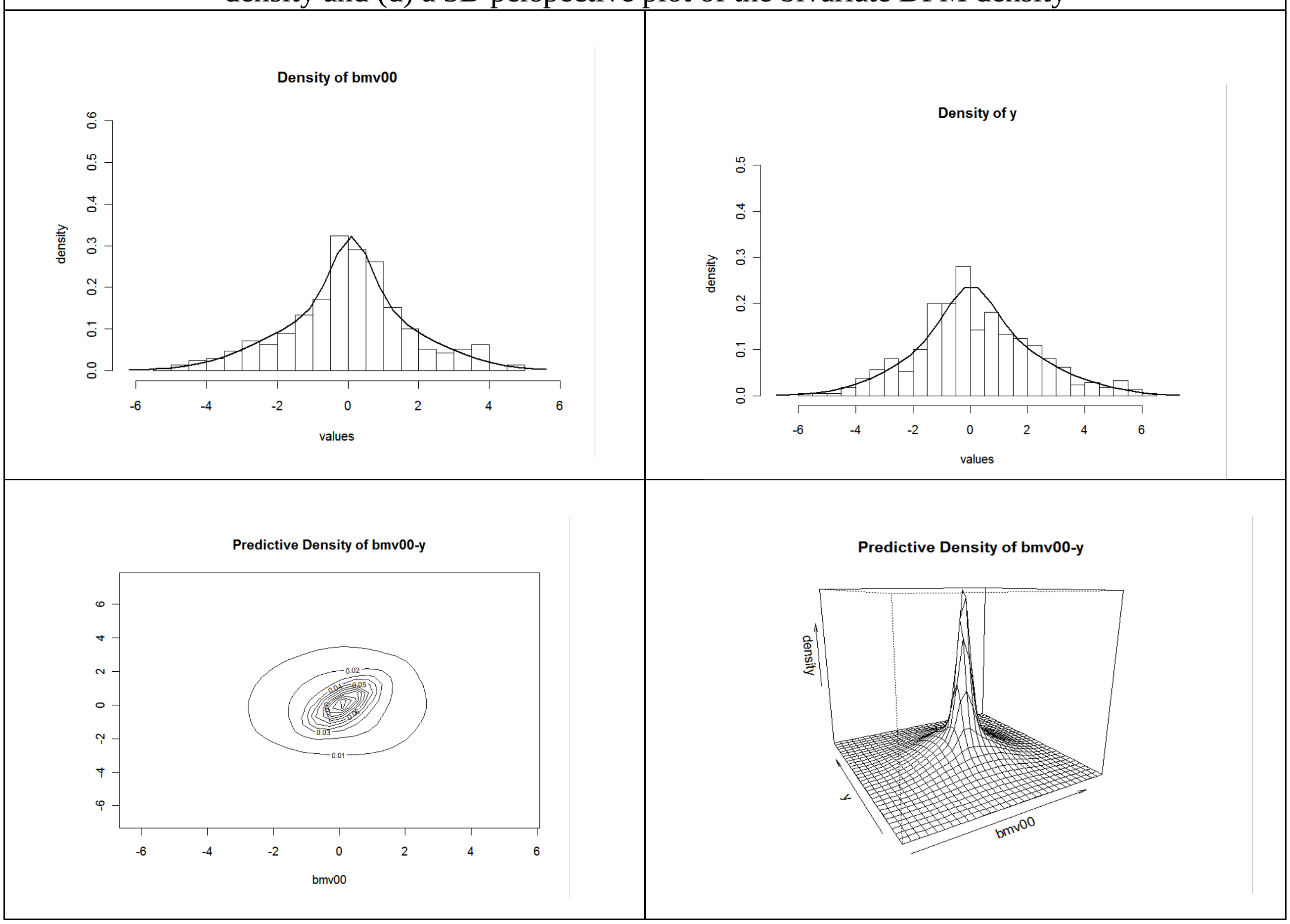

distributions are symmetric with no evidence of multimodality. The contour plot is oval and the 3D perspective plot is smooth.

Figure 7 displays the results for the most extreme data set, one with a 90 degree wedge. The marginal distributions show strong evidence of bimodality and asymmetry. The contour plot shows not only the bimodality, but also suggest that even a simple mixture of two processes would have difficulty modeling the asymmetry of the spatial intensity. The 3D perspective plot shows the two peaks quite clearly. The asymmetry of a gradual increase on the side opposite the wedge and the sharp increase on the side where the wedge models what we would expect. For the most part, there doesn't seem to be a lot of overshoot or "ringing" which is often observed when one is attempting to model a spatial density with an abrupt transition.

Figure 7: The estimated posterior density for a visual field plot with a 90^{o} wedge (a) the marginal density of x (b) the marginal density of y (c) a contour plot of the bivariate density and (d) a 3D perspective plot of the bivariate

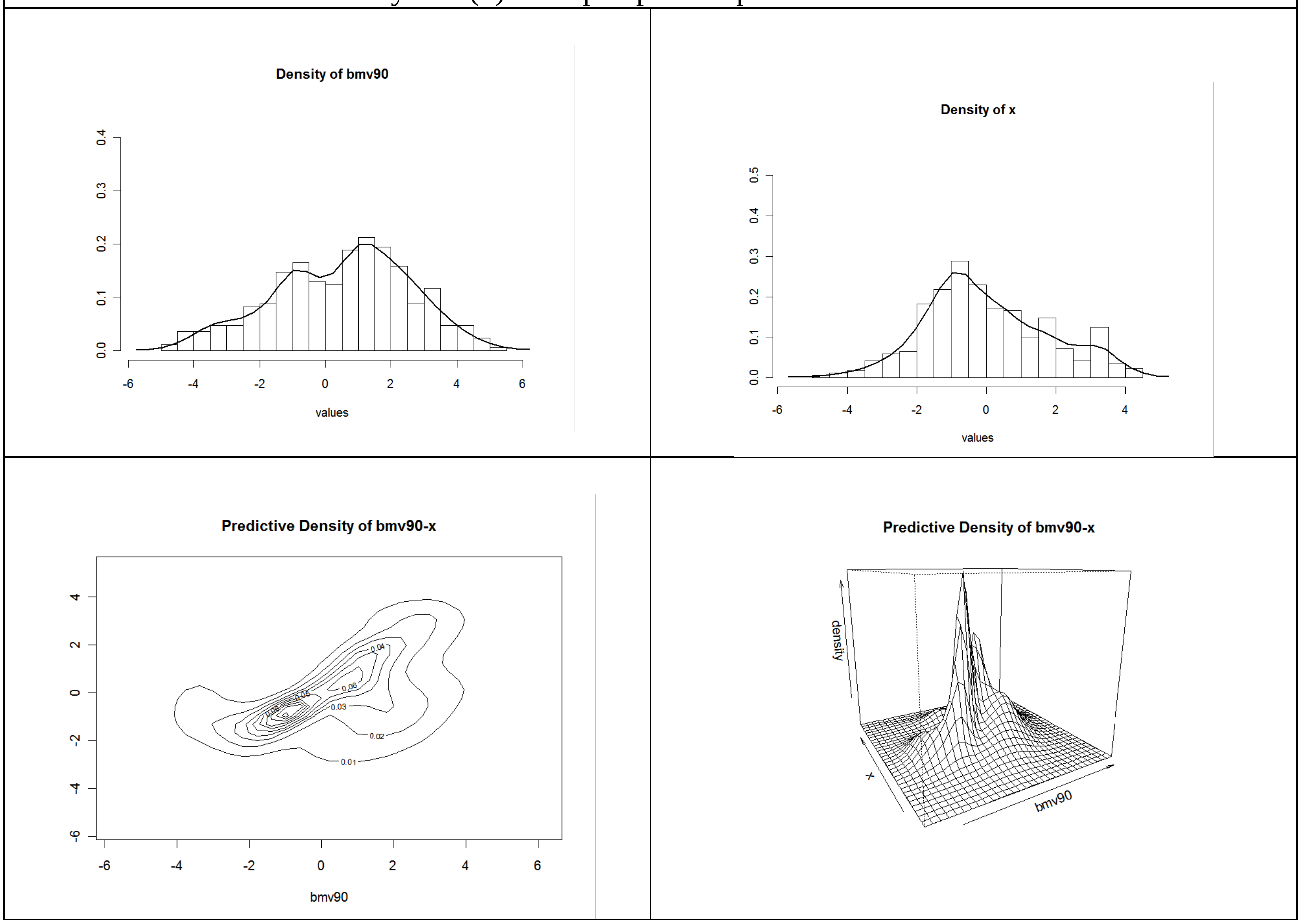

Figure 8 demonstrates that even with a smaller wedge, the DPP has the ability to detect differences in the underlying intensity. There are multiple peaks in the estimated spatial intensity. The 3D perspective plot displays this quite clearly.

Figure 8: The estimated posterior density for a visual field plot with a 36^{o} wedge
(a) the marginal density of x (b) the marginal density of y (c) a contour plot of the bivariate density and (d) a 3D perspective plot of the bivariate

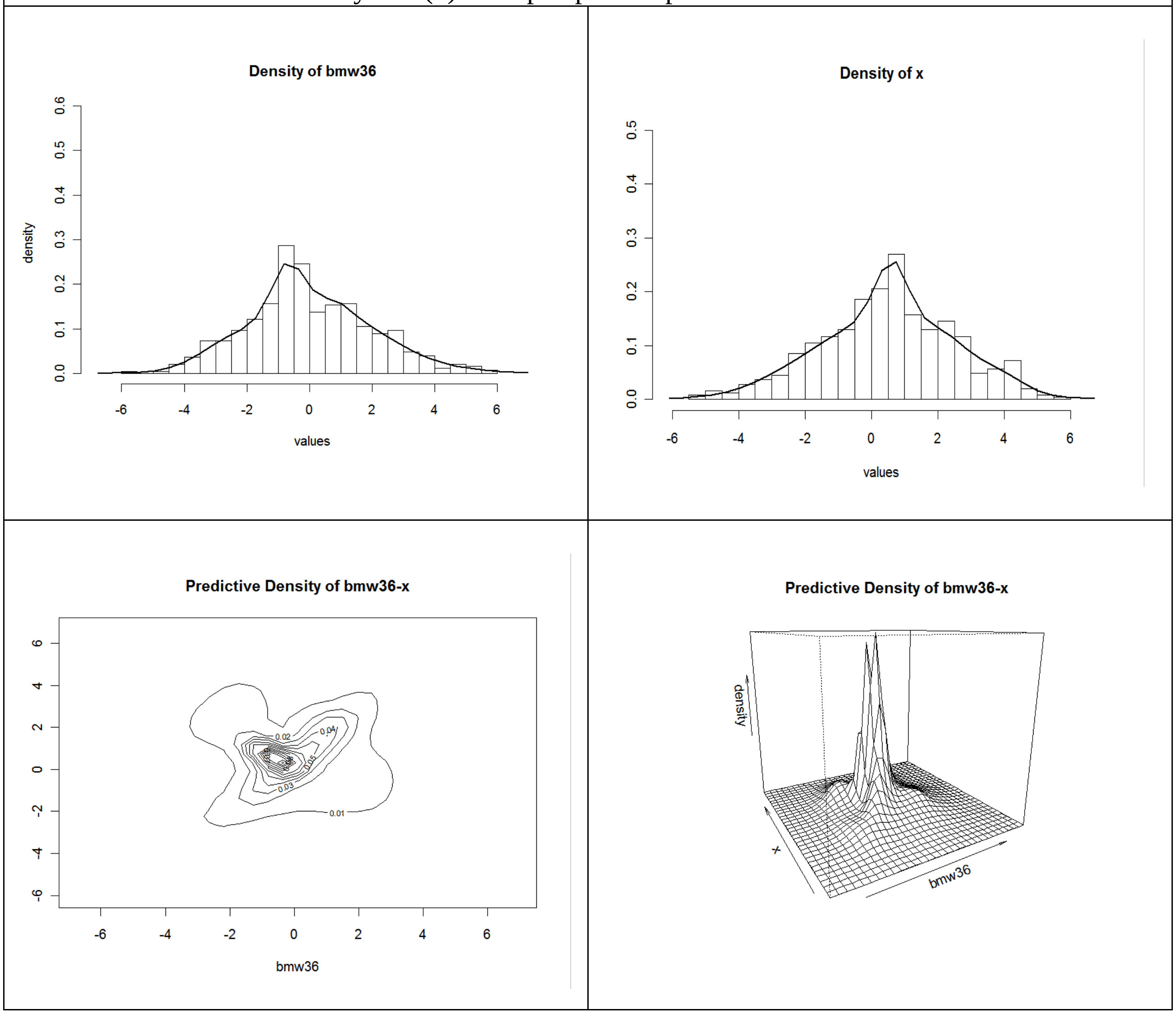

4. Discussion

The use of the DDP to estimate the posterior intensity of a point process is quite flexible. The DDP has the ability to bridge the shape from a Gaussian to a quite irregular intensity

An important question is whether these results are robust to the shape of the underlying distributions that are chosen. The DPpackage makes it possible to address this question; however, we have not yet examined how much the choice of the basis distribution affects the results.

The next step is to examine the ratio of the posterior densities under the different masks to estimate the posterior probability of a change.

Acknowledgements

Supported in part by NCRR-00058, the Medical College of Wisconsin GCRC.

References

Albert J. Bayesian Computation with R.. Springer, 2007.

Brefczynski J, DeYoe EA “A physiological correlate of the ‘spotlight’ of visual attention”. Nature Neuroscience 4:370 ff. 1999

Diggle PJ and Ribeiro PJ, Model-based Geostatistics. Springer, 2007.

Duan JA, Guindani M and Gelfand AE. “Generalized spatial Dirichelt process models“. Biometrika 94:809-825, 2007.

Gelfand J, Bayesian “Nonparametric Spatial Modeling with Dirichlet Process Mixing”. JASA, 2005. 100:1021-1035.

Hoffmann RG, Hoffmann TJ, Deyoe EA, Rowe DB. “Estimation of Pre-Post Surgical Changes in the fMRI Visual Field Map” In *JSM Proceedings*, Statistical Computing Section. Alexandria, VA. 2007.

Rizzo, ML. Statistical Computing with R. CRC Press, New York. 2008.